o-PHTHALALDEHYDE CROSS-LINKED CHITOSAN MEMBRANE AS A QUASI-SOLID-STATE ELECTROLYTE FOR SUPERCAPACITORS

Krzysztof Nowacki[1,a,*], Maciej Galiński[1,b]

[1] – Institute of Chemistry and Technical Electrochemistry, Faculty of Chemical Technology, Poznan University of Technology, Berdychowo 4 Str., 60-965 Poznań, Poland
[a] – ORCID: 0000-0002-3664-5463, [b] – ORCID: 0000-0002-0398-5760
[*]corresponding author: krzysztof.nowacki@put.poznan.pl

Abstract

This study reports a stepwise formation method of a chitosan membrane cross-linked with o*-phthalaldehyde and its use as a polymer matrix in a quasi-solid-state-electrolyte-based supercapacitor. The proposed method of cross-linking in chitosan solution and evaporation of the solvent yielded a homogeneous and durable chitosan-*o*-phthalaldehyde membrane, which, after dipping in an aqueous 2 M lithium sulfate solution, formed a quasi-solid-state-electrolyte (CS/OPAQSSE). The prepared CS/OPA-QSSE was then used in an electric double layer capacitor (EDLC) cell to study its electrochemical properties. The electrochemical performance of the EDLC cell was determined by using the electrochemical impedance spectroscopy, cyclic voltammetry and galvanostatic charging/discharging techniques. The results showed that the EDLC cell with the CS/OPA-QSSE is a fully functional and efficient device. The specific capacitance values calculated for the CS/OPA-QSSE EDLC (up to 115 F g^{-1}) always surpassed the reference cell based on a commercial glass fibre separator Therefore, the proposed chitosan modification can be considered as a future alternative to produce other polysaccharide-based materials for electrochemical use.*

Keywords: *chitosan,* o*-phthalaldehyde, quasi-solid-state electrolyte, hydrogel electrolyte, electric double-layer capacitor, supercapacitor*

Received: 27.02.2024
Accepted: 06.04.2024

1. Introduction

To meet the newest strict environmental regulations [1–3], both science and technology are becoming even more focused on the potential use of renewable materials in all fields. The reasonable demands of sustainable chemistry to design energy storage devices has led to the recognition of polysaccharides as a promising option for the replacement of components made from conventional polymer materials [4, 5]. Among them is the highly abundant marine polysaccharide chitin, which has been widely studied for its nontoxicity, biodegradability and biocompatibility [6, 7]. At the same time, chitosan (CS, the derivative of chitin), which shows good solubility in aqueous solvents, has attracted even more attention in hydrogel science due to its ease of processing and chemical modification [8, 9]. Unfortunately, to form dimensionally stable and mechanically durable CS-based hydrogels, this aminopolysaccharide has to be cross-linked [8–11]. Among all varieties of CS cross-linkers, the dialdehydes (e.g. glutaraldehyde and glyoxal) are the most widely used because permanent imine bonds can be formed easily with the neighbouring CS polymeric chains [12, 13]. Despite the dominance of glutaraldehyde as the most common modifier of CS, using different types of CS cross-linking agents may impact the hydrogel physicochemical properties; therefore, it is possible to tailor the CS hydrogel for different applications by simply changing its cross-linker [14, 15].

In the electrochemical capacitor research field, one of the leading innovations developed to increase the electrochemical performance of these devices is a quasi-solid-state electrolyte (QSSE) [16, 17]. These solid polymer matrices have a liquid electrolyte trapped inside the polymer chain interspaces and use polysaccharides of natural origin (e.g. chitin, cellulose and CS) as a matrix and an aqueous solution of inorganic salt as the dispersed phase. They represent a promising green alternative to conventional solid polymer electrolytes [18, 19]. CS hydrogels have been reported as QSSEs for supercapacitors; they exhibit good electrochemical properties and specific capacitance, even superior to devices with commercially used separators [20]. Moreover, the CS cross-linker type exerts a significant influence on electrochemical capacitor performance [21].

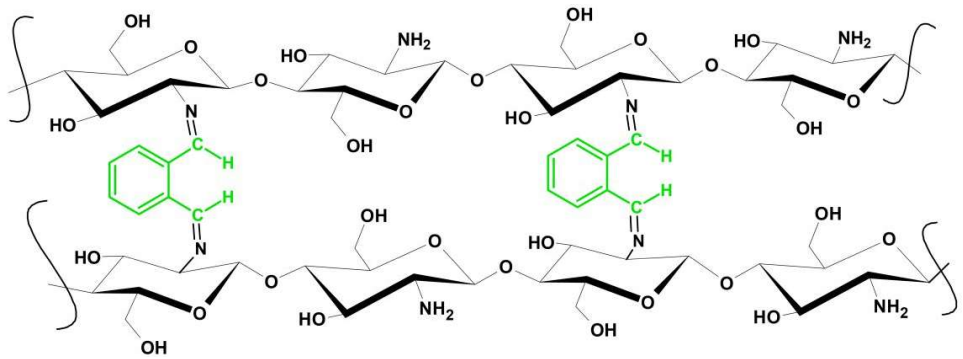

Figure 1. Schematic illustration of chitosan chemical cross-linking using *o*-phthalaldehyde [22].

This study aimed to develop an electrochemical capacitor employing a QSSE based on *o*-phthalaldehyde (OPA) cross-linked CS matrix and an aqueous lithium sulfate ($LiSO_4$) solution as a dispersed phase. It tested the hypothesis that OPA represents a replacement for glutaraldehyde in terms of cross-linking of the CS matrix (Figure 1) and that the introduction of the aromatic ring with delocalised electrons into

the biopolymer chains interspaces exerts a positive impact on the electrochemical performance of a QSSE-based supercapacitor. The prepared supercapacitor device was evaluated with advanced electrochemical methods and compared with a reference cell containing a commercial separator.

2. Materials and Methods

2.1. Chemicals

Medium-molecular-weight CS in the form of flakes was purchased from Sigma-Aldrich (USA) and dried before use (72 h at 105°C). This polysaccharide had a degree of deacetylation of 83% ± 3% and viscosity of 3.6 cP in a 2 wt% solution in 1% acetic acid (25°C). OPA (≥ 99.0%) was purchased from Sigma-Aldrich and used for CS cross-linking. Acetic acid (≥ 99.5%) and anhydrous Li_2SO_4 (≥ 98.5) were also procured from Sigma-Aldrich and used as received. Moreover, re-distilled water was used to prepare all aqueous solutions.

2.2. Preparation of *o*-Phthalaldehyde Cross-linked Chitosan Matrix

A CS-based membrane modified by OPA was used to synthesise a QSSE as a polymer matrix and prepared as follows (Figure 2). First, a 2 wt% CS solution in 1 wt% aqueous acetic acid was prepared by dispersing an appropriate quantity of dry CS flakes in acetic acid. The mixture was stirred at 37°C for 7 days to obtain a transparent, yellowish solution without solid residues. Next, the cross-linking process was initiated by mixing 6 g of homogeneous CS solution with 0.68 g of 0.10 wt% aqueous OPA solution (to obtain 0.5×10^{-5} mol of OPA) and stirred for 1 h at 25°C. The homogeneous solution was hot-cast on a poly(propylene) plate and incubated for 24 h at 37°C to evaporate the solvent.

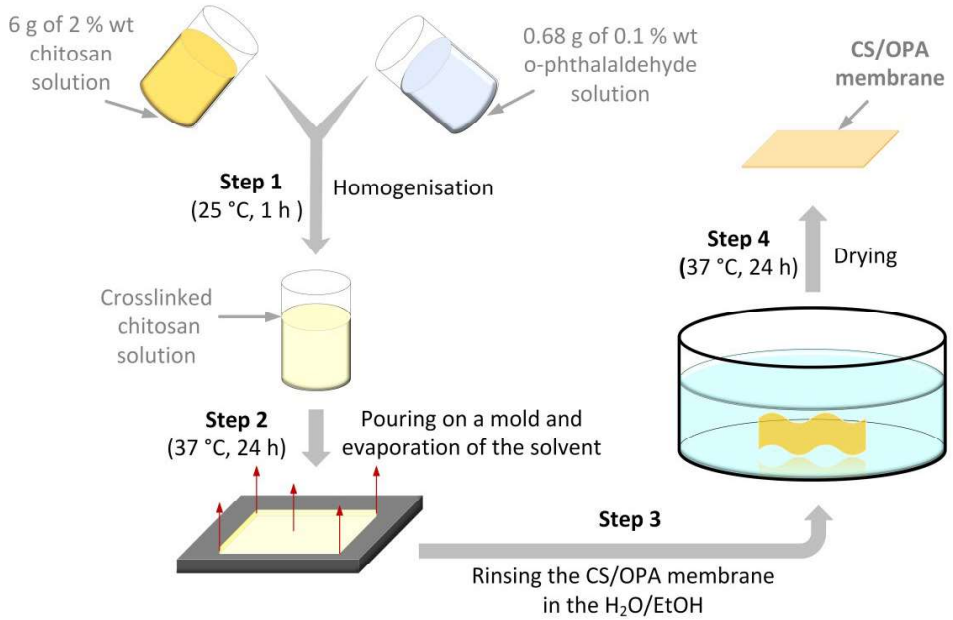

Figure 2. Preparation of the *o*-phthalaldehyde cross-linked chitosan membrane (CS/OPA).

This process yielded a slightly blurred, yellow CS/OPA membrane. It was carefully immersed in a water–ethanol bath (1:3, v/v) to remove acetic acid residues and redundant OPA particles and then dried for 24 h at 37°C.

2.3. Preparation of an *o*-Phthalaldehyde Cross-Linked Chitosan Membrane Quasi-Solid-State Electrolyte

The CS/OPA-QSSE was prepared by immersing a dry CS/OPA matrix in a 2 M Li_2SO_4 aqueous solution for 24 h at 25°C. After the incubation, the hydrogel electrolyte was carefully removed.

2.4. Attenuated Total Reflectance Fourier-Transform Infrared Spectroscopy

Attenuated total reflectance Fourier-transform infrared (ATR-FTIR) spectroscopy was used to identify possible changes in the CS polymer chain functional groups caused by cross-linking by OPA; this technique enables the non-destructive examination of the sample. ATR-FTIR spectra were recorded on a Vertex 70 Series FTIR spectrometer (Bruker, Germany) with a wave number range of 4000–500 cm^{-1} (resolution of 1 cm^{-1}). Before examination, the samples were dried to the constant mass at 37°C.

2.5. Atomic Force Microscopy

The topography and nanomechanical properties of the dry CS/OPA membrane were determined using atomic force microscopy (AFM). The three-dimensional images of the sample surface were recorded with an NX10 microscope (Park Systems, South Korea). The examined surface area was 20 × 20 μm, scanned with 512 lines per image and an non-contact mode scan speed set at approximately 0.3–0.4 Hz. The nanomechanical properties (adhesion force, energy dissipation and Young's modulus) of the dry CS/OPA membrane were examined in the PINPOINT™ mode. All measurements were performed at 23°C, and the resulting data were analysed using the open-source Gwyddion software and XEI (Park Systems) AFM analysis programs.

2.6. Contact Angle Measurements

The wettability and surface free energy of the dry CS/OPA membrane were examined by static contact angle measurements, with ethylene glycol and diiodomethane as the polar and dispersion components, respectively. Measurements were made using a sessile drop technique at 25°C with a DSA100E Drop Shape Analyzer (KRÜSS, Germany). The surface free energy was calculated using the Owens–Wendt–Rabel–Kaelble model.

2.7. Swelling Test

The degree of swelling (DS) of the CS/OPA membrane in an aqueous environment was determined using a 2 M Li_2SO_4 aqueous solution. First, a 10-mm disc was cut out from the dry CS/OPA membrane and weighed with an analytical scale (model AS 110.R2, Radwag, Poland). Next, the sample was soaked in 2.0 cm^3 of a 2 M Li_2SO_4 aqueous solution for 94 h. After specified times (10, 20 and 30 min, and 1, 2, 4, 8, 24, 48 and 96 h), the sample was removed from the electrolyte, carefully cleaned of the excess surface liquid with filter paper and weighed. DS was calculated using equation (1):

$$DS = \frac{m_w - m_d}{m_d} \times 100\% \quad (1)$$

where m_w is the mass of the wet sample and m_d is the mass of the dry sample. All measurements were performed at 23°C.

2.8. Ionic Conductivity Measurements

The ionic conductivity of the CS/OPA-QSSE was investigated with electrochemical impedance spectroscopy (EIS). The CS/OPA-QSSE sample (a disc with a diameter of 5 mm) in the equilibrium state after swelling in a 2 M Li_2SO_4 aqueous solution for 24 h was placed between two platinum blocking electrodes within a test vessel (a detailed description of the ionic conductivity test vessel is included in a previous publication [23]). All measurements were performed at 25°C and in a frequency range from 100 kHz to 1 Hz with a potential amplitude of 10 mV. The ionic conductivity (σ) of the investigated CS/OPA-QSSE was calculated using equation (2):

$$\sigma = \frac{t_S}{A \times R} \tag{2}$$

where t_s is the thickness of the swollen QSSE, A is the surface area of the working electrode (0.0177 cm^2) and R is the resistance of the sample.

2.9. Assembly of an Electric Double Layer Capacitor Test Cell

The applicability of the CS/OPA-QSSE as a hydrogel electrolyte for supercapacitors was evaluated in an electric double layer capacitor (EDLC) test cell. The symmetric EDLC cell was assembled using a two-electrode vessel produced by Swagelok (USA) (Figure 3).

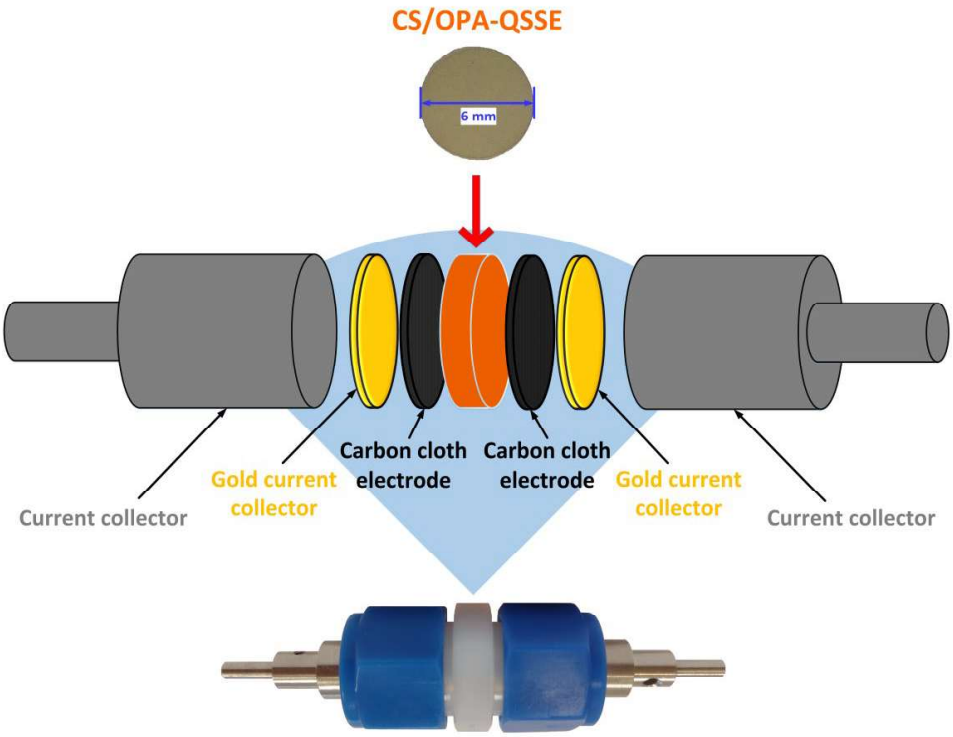

Figure 3. Schematic view of the electric double-layer capacitor assembled in this study using the Swagelok® system. Abbreviation: CS/OPA-QSSE, *o*-phthalaldehyde cross-linked chitosan membrane quasi-solid-state electrolyte.

Activated carbon cloth (2000 m^2 g^{-1}, No ACC-507-20, Kynol, Japan) and gold discs were used as electrodes and current collectors, respectively. The electrodes were shaped

as discs (diameter = 6 mm), and the mass of a single electrode was 4.8 mg; the CS/OPA-QSSE was also cut into 6-mm discs and placed between them. The reference EDLC cell with a commercial glass fibre separator (pore diameter = 1.6 µm and thickness = 0.3 mm, Whatman GF/A, UK) was assembled using the same electrode material, 2 M Li_2SO_4 solution as a liquid electrolyte and a two-electrode Swagelok vessel.

2.10. Electrochemical Measurements

The EDLC cell electrochemical performance was examined with various advanced electrochemical techniques, including electrochemical impedance spectroscopy (EIS), cyclic voltammetry (CV) and galvanostatic charge/discharge (GCD). EIS was performed using a µAutoLab FRA2 type III electrochemical system (EcoChemie, the Netherlands) in the frequency range from 100 kHz to 0.01 Hz, with a sinusoidal excitation signal of amplitude 10 mV. CV measurements were realised using the same electrochemical system in the potential range of 0–0.8 V and with different scan rates (5–100 mV s^{-1}). GCD was carried out at a constant current of 5 mA with the cell voltage stepped from 0 to 0.8 V, using a Interface 5000 (Gamry Instruments, USA). All electrochemical measurements were performed at 25°C.

3. Results and Discussion

3.1. Attenuated Total Reflectance Fourier-Transform Infrared Spectroscopy

Figure 4 presents the ATR-FTIR spectra obtained for CS standard powder and the CS/OPA membrane.

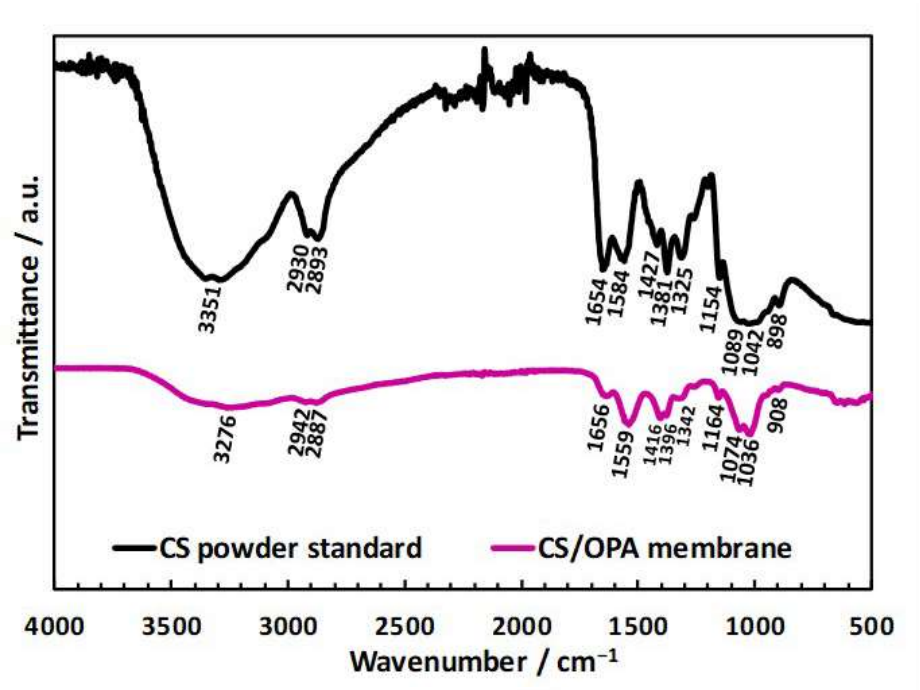

Figure 4. Attenuated total reflectance Fourier-transform infrared spectra of chitosan standard powder (CS, black curve) and the chitosan/*o*-phthalaldehyde (CS/OPA) membrane (purple curve).

The reference sample spectrum (Figure 4, black curve) features characteristic bands for CS, including amide I at 1654 cm^{-1} (νC═O), amide III at 1325 cm^{-1} (νC—N) and the band at around 898 cm^{-1} (νC—O—C bridge) [14, 24, 25]. Moreover, there is a distinctive band at 1584 cm^{-1} attributed to the N—H in-plane bending vibrations of the primary amine group. A detailed analysis of the CS/OPA membrane spectrum (Figure 4, purple line) reveals absorption peaks that correspond with the reference sample. However, their wavelengths are shifted slightly and the intensity is markedly lower, which is a frequent phenomenon observed in the spectra of heavily processed CS materials [8, 14, 21, 24, 25]. The cross-linking process caused significant changes in both the wavelength and intensity of the band at 1559 cm^{-1}, which most probably corresponds to the amide II (δN—H) vibrations of the residual *N*-acetyl groups [24]. Such a band confirms the imine bond formation between CS polymeric chains and OPA. In this reaction, the amine groups are consumed (Figure 1); thus, the characteristic band of amide II (overlapped in the reference sample spectrum by the δNH_3^+ vibrations of the primary amine group) can be distinguished.

3.2. Atomic Force Microscopy Characterisation

The topography of the CS/OPA membrane in the dry state and the nanomechanical properties were examined with AFM (Figure 5). The thickness of the investigated sample in the dry state was 30 ± 1 μm.

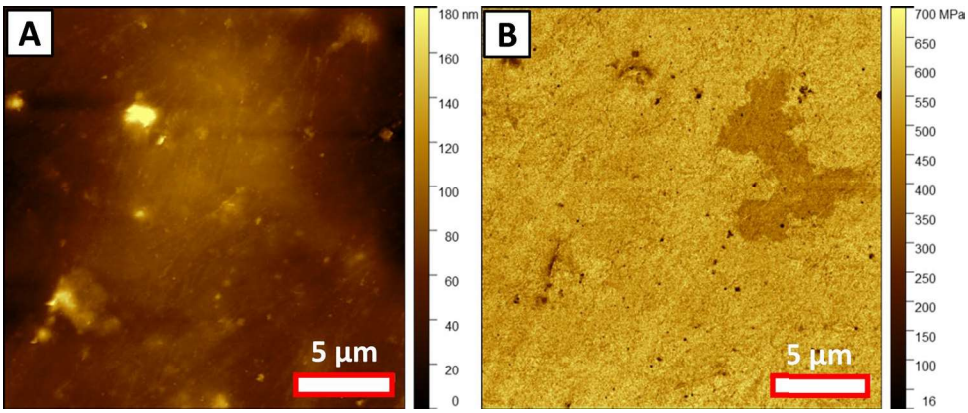

Figure 5. The atomic force micrographs show (A) the surface topography of the chitosan/*o*-phthalaldehyde membrane and (B) the distribution of Young's modulus on the membrane surface.

The general topography of the CS/OPA membrane (Figure 5A) shows a relatively homogeneous and fine-grained surface with an average height of 64.5 nm, an average grain radius of 64.5 ± 2.8 nm and a mean roughness parameter of 30.74 nm, which are within the wide range of published values for various cross-linked CS membranes [9, 26, 27]. However, a few higher spots are visible (Figure 5A), and the maximum height analysis yielded an h_{max} value of 258.1 nm, which may be caused by the presence of insoluble residues of biomineralised crustacean shell or micro air bubbles congealed during the solvent evaporation process.

The nanomechanical properties – adhesion force, energy dissipation and Young's modulus – were also investigated. The average adhesion force and energy dissipation were 1.85 ± 0.21 nN and 0.85 ± 0.03 fJ, respectively. Young's modulus showed a relatively

regular distribution of values across the captured image (Figure 5B), with an average of 512.0 ± 2.2 GPa. Further detailed analysis revealed that similarly to the topography image, there are a few areas characterised with lower Young's modulus on the membrane surface. Interestingly, these areas correspond to the spots of inhomogeneity found across the topography image (Figure 5A) and suggest that even small solid inclusions within the CS-based membrane may impact the polymer matrix's mechanical properties.

3.3. Surface Free Energy

Measurement of the contact angle is widely used to determine the wettability of polymer membranes and matrices [23, 28]. In the present study, it was measured to obtain a preliminary evaluation of the applicability of the CS/OPA matrix in polar and non-polar liquid electrolytes. Figure 6 presents a detailed view of the contact angles and shapes of liquid droplets (ethylene glycol and diiodomethane) on the CS/OPA membrane.

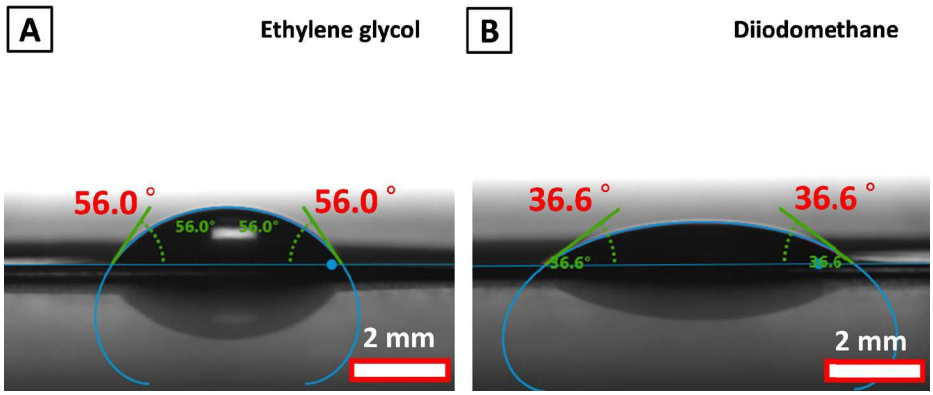

Figure 6. Estimated equilibrium contact angles for the chitosan/*o*-phthalaldehyde membrane with (A) ethylene glycol and (B) diiodomethane as a drop of liquid.

The drop shape analysis revealed that the CS/OPA membrane was well wetted by the non-polar liquid (Figure 6B, contact angle = 36.6°) and wetted slightly less by the polar liquid (Figure 6A, contact angle = 56.0°). Because unmodified CS membranes are often characterised in the literature as extremely wettable by water, it can be assumed that cross-linking CS with OPA decreased its hydrophilic character [8, 9, 21, 28]. The surface free energy dispersive and polar components calculated for the CS/OPA membrane (41.8 and 0.7 mN m^{-1}, respectively) also confirmed that covalent cross-linking of CS reduced its hydrophilicity, possibly by due to the increase in London forces [8, 29]. Thus, the results suggest that CS cross-linked with OPA might be applied for both aqueous and non-aqueous electrolyte systems and simultaneously eliminate the excessive swelling hazard.

3.4. Degree of Swelling and Ionic Conductivity Measurements

The electrolyte uptake test (25°C, 2 M Li_2SO_4) provided essential data for evaluating the effectiveness of the cross-linking process and possible application of the CS/OPA membrane as a QSSE polymer matrix. The non-cross-linked CS membrane was utilised as a reference sample, and the results of this test are shown in Figure 7. Analysis of the DS versus time dependency graph registered for the unmodified CS membrane revealed an extremely high DS (up to 250% by mass, 96 h), which unambiguously implies that without cross-linking of its polymer structure, CS is not applicable as a QSSE matrix due to the excessive swelling and possible electrolyte leakage.

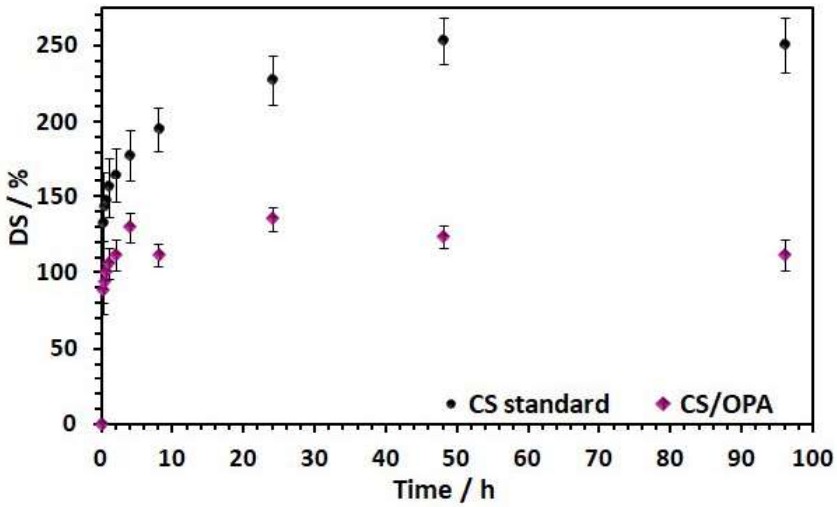

Figure 7. The degree of swelling (DS) versus time in a 2 M lithium sulfate (Li_2SO_4) aqueous solution of unmodified chitosan membrane (CS) and the chitosan/*o*-phthalaldehyde (CS/OPA) membrane.

The swelling curve obtained for the CS/OPA membrane featured a typical cross-linked CS shape, where immediately after the sample contact with neutral aqueous media, there was a dynamic increase in DS. This effect is attributed to the osmotic pressure and the diffusion of water molecules into the polymer network [26, 30]. Next, a small drop in DS can be observed, indicating the relaxation of hydrated CS chains. Finally, the polymer network expands into the solvent until swelling forces balance the osmotic pressure and the CS-based hydrogel reaches its equilibrium state [26, 27, 30]. The maximum DS measured for the CS/OPA hydrogel was 135% by mass (after 24 h), and the equilibrium DS was 112% by mass (after 96 h); both are significantly lower than the respective parameters of the reference sample (Figure 7). Therefore, the CS/OPA membrane used in this study should be recognised as a possible QSSE polymer matrix due to its well-stabilised three-dimensional polymer chain network and balanced swelling behaviour.

One of the most essential factors describing a QSSE is its ionic conductivity. A reduction in electrolyte absorption below a certain level will negatively impact this parameter [21, 31]. Table 1 presents the ionic conductivity, thickness and bulk resistance of the standard glass fibre separator soaked in the 2 M Li_2SO_4 aqueous solution and hydrogel electrolyte used in this study. Based on EIS, the ionic conductivity for CS/OPA QSSE was 26.1 S cm^{-1}, which is comparable to other polysaccharide-based hydrogel electrolytes [21, 23, 32–37].

Table 1. The ionic conductivity (σ), bulk resistance (R), thickness in the swollen state (t_s) and equivalent circuit (EC) used in the electrochemical impedance spectroscopy fitting method.

Electrolyte	σ [mS cm^{-1}]	R [Ω]	t_s [cm]	EC
CS/OPA-QSSE	26.1	15.8 ± 0.8	0.0073 ± 0.0001	$R_1(R_2CPE)$
Whatman GF/A	58.3	11.9 ± 0.4	0.0123 ± 0.0001	$R_1(R_2CPE)$

Note. Abbreviation: CS/OPA-QSSE, *o*-phthalaldehyde cross-linked chitosan membrane quasi-solid-state electrolyte.

3.5. Electrochemical Studies

The applicability of the CS/OPA-QSSE as a component of a supercapacitor was evaluated using standard electrochemical methods, namely EIS, CV and GCD. Moreover, the EDLC was selected as the best system for the electrochemical performance tests of the CS-based hydrogel electrolyte.

Figure 8A and 8B display the Nyquist plots for the CS/OPA-QSSE capacitor and the Whatman GF/A reference cell, respectively, before the GCD test. The shapes of the registered EIS spectra for both investigated devices fit well with the typical EDLC characteristics, including the ability to see the visible arc in the high-frequency area and a straight line parallel to the imaginary part of the impedance axis in the low-frequency range [16, 19, 38].

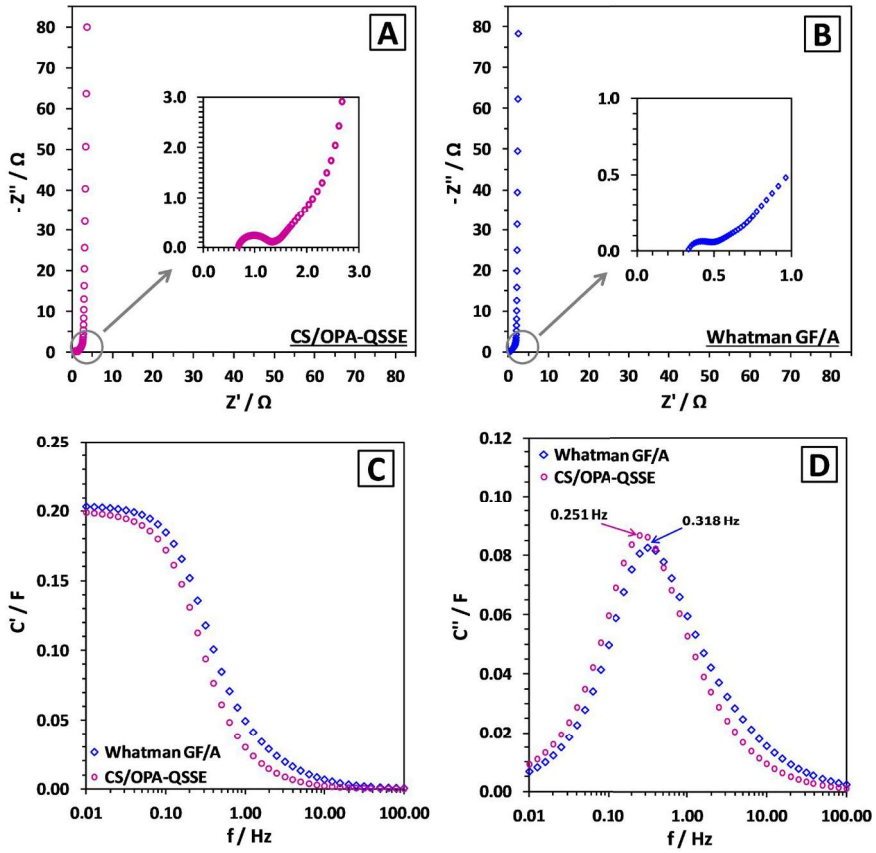

Figure 8. Nyquist plots for the electric double-layer capacitor with (A) the *o*-phthalaldehyde cross-linked chitosan membrane quasi-solid-state electrolyte (CS/OPA-QSSE) and (B) the Whatman GF/A glass fibre separator. (C) Evaluation of the real part of capacitance (C') versus frequency and (D) the imaginary part of capacitance (C'') with characteristic frequencies.

Further detailed analysis of the insets in Figure 8A and 8B provided two crucial parameters: series resistance (R_S) and charge transfer resistance (R_{CT}) [16, 39]. R_S is attributed to the resistance between the working electrode and the counter electrode within the electrochemical device; it can be calculated by extrapolating the high-frequency part of the EIS spectra to the condition Z' = 0 [16, 39]. R_{CT} is associated with the ion electron

transfer resistance across the electrode electrolyte interface; it can be extracted as the diameter of the first semi-circle within the Nyquist plot [16, 39]. Therefore, knowing both parameters provides complete information about the internal resistances within the tested EDLC. Table 2 provides the R_S and R_{CT} extracted from Figure 8A and 8B.

Table 2. Series resistance (R_S), charge transfer resistance (R_{CT}) and relaxation time constant (τ_0) extracted from electrochemical impedance spectroscopy.

Electric double-layer capacitor	R_S [Ω]	R_{CT} [Ω]	τ_0 [s]
CS/OPA-QSSE	0.7 ± 0.1	0.7 ± 0.1	4
Whatman GF/A in 2 M Li_2SO_4	0.3 ± 0.1	0.2 ± 0.1	3

Abbreviations: CS/OPA-QSSE, *o*-phthalaldehyde cross-linked chitosan membrane quasi-solid-state electrolyte.

Figure 8C and 8D show the dependence of real (C') and imaginary (C'') parts of capacitance versus frequency registered for the tested EDLCs [38]. Detailed analysis of the C''(ω) curves, including determining their peak frequencies (Figure 8D), allowed us to calculate another crucial EDLC parameter, namely the relaxation time constant (τ_0), which represents the time during EIS needed for the adsorption and desorption of electrolyte ions in the pores of carbon cloth electrodes [38, 40]. τ_0 was calculated with equation (3):

$$\tau_0 = \frac{1}{f_0} \tag{3}$$

where f_0 is the maximum of the C''(ω) curve [38, 40]. The results are presented in Table 2.

Summarising the EIS investigation, the internal resistance parameters calculated for the CS/OPA-QSSE test cell were relatively low (R_S and R_{CT} are both 0.7 ± 0.1 Ω) and comparable to the published values for other polysaccharide-based QSSEs [18, 19, 21, 23, 35–37, 41]. However, it should be noted that compared with the Whatman GF/A reference cell (R_S = 0.3 ± 0.1 Ω and R_{CT} = 0.2 ± 0.1 Ω), the resistance between the working electrode and counter electrode was nearly two times higher, a phenomenon that corresponds to diminished ionic conductivity of the CS/OPA-QSSE described earlier. Nonetheless, τ_0 was similar for both EDLCs (3 s for the reference cell and 4 s for the CS/OPA-QSSE); hence, CS/OPA-QSSE should exhibit good capacitive behaviour [16, 40].

The voltammetry curves recorded for both tested EDLCs (a sweep rate of 10 mV s^{-1} in the potential range of 0–0.8 V) are shown in Figure 9. The CS/OPA-QSSE cell exhibited the standard quasi-rectangular shape of the CV curve with no visible redox peaks and good charge propagation (Figure 9A). Thus, the non-Faradic nature of the capacitive processes during the cycling work of the device can be expected [31, 33, 35]. Interestingly, the voltammogram recorded for the Whatman GF/A reference EDLC showed nearly the same shape as the CS/OPA-QSSE cell, consistent with the relatively small differences in the internal resistances of the investigated devices based on the EIS analysis.

Figure 9B shows a comparison of voltammograms registered after 10,000 charging/discharging cycles in the potential range of 0–0.8 V. In general, the recorded CV curves maintained their box-type shape and good charge propagation even after an extended GCD test, which indicates excellent electrochemical stability of the CS/OPA-QSSE in the operational voltage range [18, 19, 21, 23, 35–37, 41].

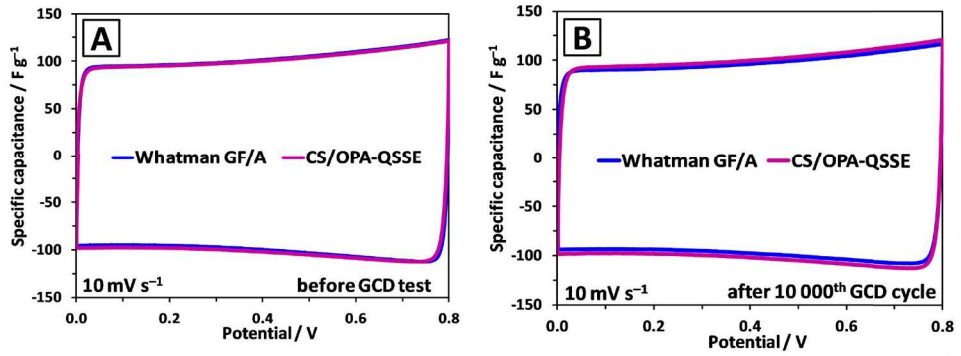

Figure 9. Comparison of the cyclic voltammetry curves recorded at the scan rate 10 mV s^{-1} (A) before the galvanostatic charge/discharge test and (B) after 10,000 charging/discharging cycles.

The cyclic repeatability and the specific discharge capacitance (C_{SP}) of the CS/OPA-QSSE and Whatman GF/A test cells were estimated with the GCD method. Figure 10A and 10B show the potential/time dependency recorded for the 1st and 10,000th charging/discharging cycles of the investigated EDLCs.

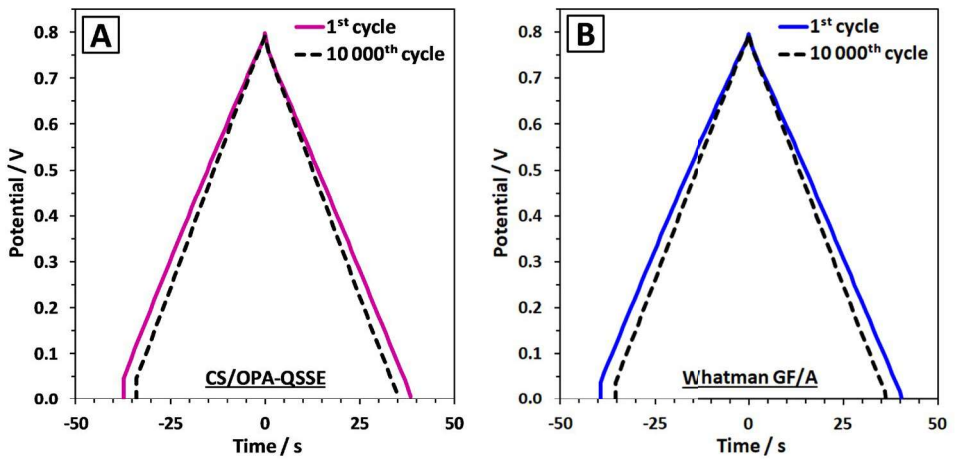

Figure 10. Galvanostatic charge/discharge curves at the 1st and 10,000th cycle for the electric double-layer capacitor test cells with the (A) *o*-phthalaldehyde cross-linked chitosan membrane quasi-solid-state electrolyte (CS/OPA-QSSE) and (B) the Whatman GF/A glass fibre separator.

All registered GCD profiles exhibited a symmetric and triangular shape for both the 1st and 10,000th cycle. This is a typical characteristic of EDLCs, which indicates the non-Faradaic nature of the capacitive processes within the device [33, 35, 41]. Unfortunately, the last GCD profile captured for the CS/OPA-QSSE EDLC did not overlap the initial one, which suggests that the cyclic repeatability of the CS/OPA-QSSE device will be slightly diminished. Nonetheless, the observed

phenomenon (manifested by narrowing the triangle base of the GCD profile) also occurred for the Whatman GF/A reference cell; therefore, it can be considered a frequent EDLC problem caused by clogging of the electrode material pores [42].

Thus, the GCD curves of the CS/OPA-QSSE test cell (Figure 10A) do not depart from the reference cell GCD characteristic (Figure 10B). Because both feature relatively low ohmic drops, their specific capacitance (CSP) can be calculated from equation (4):

$$C_{SP} = \frac{I}{\frac{\mathrm{d}U}{\mathrm{d}t} \times m_{el}} \tag{4}$$

where I is the discharge current, $\mathrm{d}U/\mathrm{d}t$ is the slope of the discharge curve and m_{el} is the total mass of the active electrode material.

The CS/OPA-QSSE test cell exhibited the highest specific discharge capacitance values for the 1st and 10,000th cycles (115 and 103 F g^{-1}, respectively). Although the specific discharge capacitance was slightly lower for the Whatman GF/A cell (113 and 101 F g^{-1} for the 1st and 10,000th cycles, respectively), the electrochemical performance of both EDLCs may be described as comparable with previous data published for analogous systems [33, 37].

Figure 11 provides a visualisation of the repeatability of the CS/OPA-QSSE EDLC. There was good cyclic stability of the investigated capacitors. The CS/OPA-QSSE and Whatman GF/A capacitors had relatively high capacitance retention (89.6% and 89.4%, respectively) [19, 28, 40, 41].

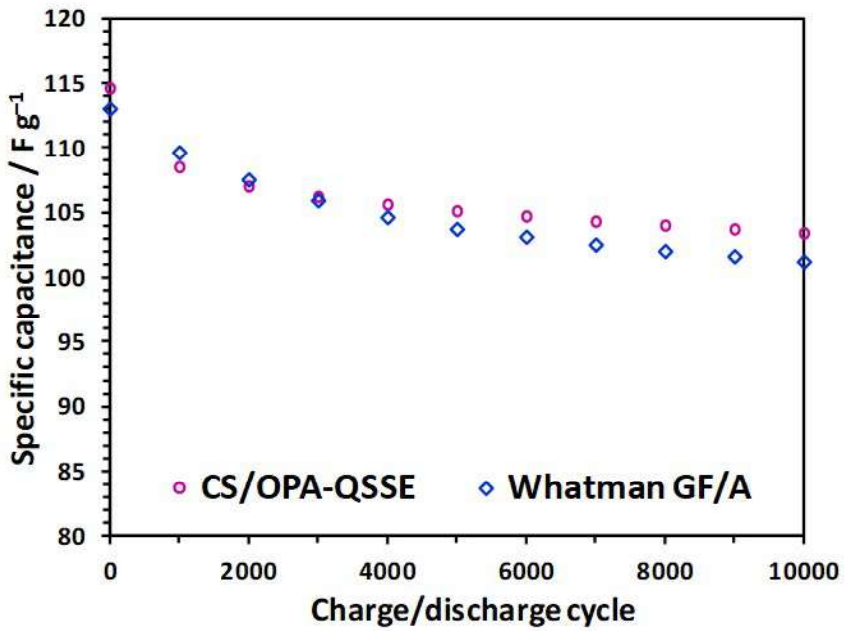

Figure 11. Cyclic stability of the tested electric double-layer capacitors over 10,000 galvanostatic charge/discharge cycles. Abbreviation: CS/OPA-QSSE, *o*-phthalaldehyde cross-linked chitosan membrane quasi-solid-state electrolyte.

Conclusively, the GCD investigation of the CS/OPA-QSSE as a component of a supercapacitor proves that despite its lower ionic conductivity (over two times lower than for the reference separator material), the electrochemical performance of the EDLC that contains it was comparable to the reference cell with a commercial glass fibre separator. These results also suggest that OPA as a CS cross-linker is electrochemically stable (within the 0–0.8 V potential window) and does not cause redox reactions within QSSE. Based on a review of the literature (Table 3), the electrochemical properties of the investigated CS/OPA-QSSE capacitor are in the range of previously published data. Moreover, the specific capacitance calculated for the CS/OPA-QSSE EDLC surpasses the majority of other reported cells with similar architecture.

Table 3. Electrochemical performance of the electric double-layer capacitor systems with the quasi-solid-state-electrolytes based on chitosan matrix reported in the literature.

Polymer matrix	Modifier	Dispersed phase	σ [mS cm^{-1}]	Voltage window [V]	CSP [F g^{-1}]	Ref
Chitosan	*o*-Phthalaldehyde	$Li_2SO_{4(aq)}$	26.1	0–0.8	115 (103)	This work
Chitosan	Glutaraldehyde	$CH_3COOLi_{(aq)}$	13.0	0–0.8	106.0	[21]
Chitosan	NaOH	$CH_3COOLi_{(aq)}$	14.3	0–0.8	106.0	[21]
Chitosan	Chitin	$CH_3COOLi_{(aq)}$	-	0–0.8	98.0	[43]
Chitosan	-	$Li_2SO_{4(aq)}$	39.1	0–0.8	97.0	[37]
Chitosan	Sodium alginate	$Li_2SO_{4(aq)}$	18.7	0–0.8	101.0	[37]
Chitosan	PEG/PPG	$H_2SO_{4(aq)}$	-	0–1.0	132.0	[44]
Chitosan	-	$Na_2SO_{4(aq)}$	-	0–1.6	35.0	[28]
Carboxymethyl chitosan	-	$Na_2SO_{4(aq)}$	-	0–1.8	72.5	[28]
Carboxymethyl chitosan	Acrylic acid/MBA	$KOH_{(aq)}$	75.6	0–0.9	39.1	[32]
Carboxymethyl chitosan	Acrylic acid/$fecl_3$	$KOH_{(aq)}$	47.1	0–0.9	33.5	[32]
Carboxymethyl chitosan	PAM/MBA	$Li_2SO_{4(aq)}$	17.4	0–1.4	31.9	[33]
Chitosan	PC/EC	$LiClO_{4(aq)}$	5.5	0–1.0	80.0	[34]
Carboxymethyl chitosan	-	$HCl_{(aq)}$	86.9	0–0.9	45.9	[35]
Chitosan	PAEK-g-PEG	$LiClO_{4(aq)}$	8.0	0–1.5	120.8	[36]
Chitosan	Glyoxylic acid	$KOH_{(aq)}$	-	0–0.8	95.0	[45]

4. Conclusions

A novel polysaccharide-based QSSE with a polymer matrix – CS cross-linked with OPA – was developed successfully, and a 2 M Li_2SO_4 aqueous solution was utilised as a dispersive phase. Characterisation of the physicochemical properties (using ATR-FTIR

spectroscopy, AFM and contact angle measurements) confirmed that OPA-mediated cross-linking modified the CS matrix. The CS/OPA-QSSE possessed excellent ionic conductivity and, therefore, its applicability as a hydrogel electrolyte in an EDLC was evaluated. The symmetric EDLC based on the CS/OPA-QSSE showed good electrochemical performance (without visible redox processes) and superior specific discharge capacitance (up to 115 F g^{-1}) compared with the reference cell with a commercial Whatman GF/A glass fibre separator (up to 113 F g^{-1}). This study represents the first successful realisation of OPA-cross-linked CS as a QSSE polymer matrix. It can be considered as a future alternative for other polysaccharide-based materials for electrochemical purposes.

5. Acknowledgements

This work was performed with the financial support of the Ministry of Science and Higher Education, Poland (grant no. 0911/SBAD/2402). The authors thank Marcin Wysokowski (Poznan University of Technology, Poland) for technical support during the contact angle measurements.

6. References

[1] Regulation (EU) 2023/1542 concerning batteries and waste batteries (2023). Off J L191, 1–117.

[2] Regulation (EU) 2021/1119 establishing the framework for achieving climate neutrality (2021). Off J L243, 1–17.

[3] Directive 2012/19/EU on waste electrical and electronic equipment (2012). Off J L197, 38–71.

[4] Musarurwa H, Tavengwa NT; (2022) Application of polysaccharide-based metal organic framework membranes in separation science. Carbohydr Polym 275, 118743. **DOI:**10.1016/j.carbpol.2021.118743

[5] Shen X, Shamshina JL, Berton P, Gurau G, Rogers RD; (2016) Hydrogels based on cellulose and chitin: fabrication, properties, and applications. Green Chem 18, 53–75. **DOI:**10.1039/C5GC02396C

[6] Mutsenko VV, Gryshkov O, Lauterboeck L, Rogulska O, Tarusin DN, Bazhenov VV, Schütz K, Brüggemeier S, Gossla E, Akkineni AR, Meißner H, Lode A, Meschke S, Fromont J, Stelling AL, Tabachnik KR, Gelinsky M, Nikulin S, Rodin S, Tonevitsky AG, Petrenko AY, Glasmacher B, Schupp PJ, Ehrlich H; (2017) Novel chitin scaffolds derived from marine sponge Ianthella basta for tissue engineering approaches based on human mesenchymal stromal cells: Biocompatibility and cryopreservation. Int J Biol Macromol 104, 1955–1965. **DOI:**10.1016/j.ijbiomac.2017.03.161

[7] Sahraee S, Milani JM, Ghanbarzadeh B, Hamishehkar H; (2017) Physicochemical and antifungal properties of bio-nanocomposite film based on gelatin-chitin nanoparticles. Int J Biol Macromol 97, 373–381. **DOI:**10.1016/j.ijbiomac.2016.12.066

[8] Takeshita S, Konishi A, Takebayashi Y, Yoda S, Otake K; (2017) Aldehyde approach to hydrophobic modification of chitosan aerogels. Biomacromol 18, 2172–2178. **DOI:**10.1021/acs.biomac.7b00562

[9] Gierszewska M, Ostrowska-Czubenko J; (2016) Chitosan-based membranes with different ionic crosslinking density for pharmaceutical and industrial applications. Carbohydr Polym 153, 501–511. **DOI:**10.1016/j.carbpol.2016.07.126

[10] Yu X, Zhang J, Zheng Y; (2021) Perchlorate adsorption onto epichlorohydrin crosslinked chitosan hydrogel beads. Sci Total Environ 761, 143236. **DOI:**10.1016/j.scitotenv.2020.143236

[11] Vo NTN, Huang L, Lemos H, Mellor AL, Novakovic K; (2021) Genipin-crosslinked chitosan hydrogels: Preliminary evaluation of the *in vitro* biocompatibility and biodegradation. J Appl Polym Sci 138(34), 50848. **DOI:**10.1002/app.50848

[12] Kaczmarek-Szczepańska B, Mazur O, Michalska-Sionkowska M, Łukowicz K, Osyczka AM; (2021) The preparation and characterization of chitosan-based hydrogels cross-linked by glyoxal. Materials 14, 2449. **DOI:**10.3390/ma14092449

[13] Li Q, Su H, Yang Y, Zhang J, Xia C, Guo Z; (2023) Adsorption property and mechanism of glutaraldehyde-crosslinked chitosan for removal of 2,4-dichlorophenoxyacetic acid from water. Environ Sci 9(1), 294–307. **DOI:**10.1039/d2ew00638c

[14] Acharya V, Ghosh A, Chowdhury AR, Datta P; (2021) Tannic acid-crosslinked chitosan matrices enhance osteogenic differentiation and modulate epigenetic status of cultured cells over glutaraldehyde crosslinking. Soft Mater 20, 149–160. **DOI:**10.1080/1539445X.2021.1933032

[15] Jóźwiak T, Filipkowska U, Szymczyk P, Rodziewicz J, Mielcarek A; (2017) Effect of ionic and covalent crosslinking agents on properties of chitosan beads and sorption effectiveness of Reactive Black 5 dye. React Funct Polym 114, 58–74. **DOI:**10.1016/j.reactfunctpolym.2017.03.007

[16] Hor AA, Yadav N, Hashmi S; (2023) Enhanced energy density quasi-solid-state supercapacitor based on an ionic liquid incorporated aqueous gel polymer electrolyte with a redox-additive trimethyl sulfoxonium iodide. J Energy Storage 64, 107227. **DOI:**10.1016/j.est.2023.107227

[17] Fan L, Tu Q, Geng C, Huang J, Gu Y, Lin J, Huang Y, Wu J; (2020) High energy density and low self-discharge of a quasi-solid-state supercapacitor with carbon nanotubes incorporated redox-active ionic liquid-based gel polymer electrolyte. Electrochim Acta 331, 135425. **DOI:**10.1016/j.electacta.2019.135425

[18] Lin X, Wang M, Zhao J, Wu X, Xie J, Yang J; (2023) Super-tough and self-healable all-cellulose-based electrolyte for fast degradable quasi-solid-state supercapacitor. Carbohydr Polym 304, 120502. **DOI:**10.1016/j.carbpol.2022.120502

[19] Çevik, E, Günday ŞT, Bozkurt A, Iqbal A, Asiri SM, Alqarni AN, Almofleh A; (2022) Scalable, quasi-solid-state bio-polymer hydrogel electrolytes for high-performance supercapacitor applications. ACS Sustain Chem Eng 10(33), 10839–10848. **DOI:**10.1021/acssuschemeng.2c02281

[20] Roy BK, Tahmid I, Rashid TU; (2021) Chitosan-based materials for supercapacitor applications: a review. J Mater Chem A 9(33), 17592–17642. **DOI:**10.1039/d1ta02997e

[21] Nowacki K, Galiński M, Stępniak I; (2019) Synthesis and characterization of modified chitosan membranes for applications in electrochemical capacitor. Electrochim Acta 320, 134632. **DOI:**10.1016/j.electacta.2019.134632

[22] Garg M, Bhullar N, Bajaj B, Sud D; (2021) Terephthalaldehyde as a good crosslinking agent in crosslinked chitosan hydrogel for the selective removal of anionic dyes. New J Chem 45(11), 4938–4949. **DOI:**10.1039/d0nj05758d

[23] Wysokowski M, Nowacki K, Jaworski F, Niemczak M, Bartczak P, Sandomierski M, Piasecki A, Galiński M, Jesionowski T; (2022) Ionic liquid-assisted synthesis of chitin-ethylene glycol hydrogels as electrolyte membranes for sustainable electrochemical capacitors. Sci Rep 12(1), 8861. **DOI:**10.1038/s41598-022-12931-w

[24] Weißpflog J, Vehlow D, Müller M, Kohn B, Scheler U, Boye S, Schwarz S; (2021) Characterization of chitosan with different degree of deacetylation and equal viscosity in dissolved and solid state – insights by various complimentary methods. Int J Biol Macromol 171, 242–261. **DOI:**10.1016/j.ijbiomac.2021.01.010

[25] Klein MP, Hackenhaar CR, Lorenzoni ASG, Rodrigues RC, Costa TMH, Ninow JL, Hertz PF; (2016) Chitosan crosslinked with genipin as support matrix for application in food process: support characterization and β-d-galactosidase immobilization. Carbohydr Polym 137, 184–190. **DOI:**10.1016/j.carbpol.2015.10.069

[26] Ostrowska-Czubenko J, Gierszewska M, Pieróg M; (2015) pH-responsive hydrogel membranes based on modified chitosan: water transport and kinetics of swelling. J Polym Res 22(8), 153. **DOI:**10.1007/s10965-015-0786-3

[27] Węgrzynowska-Drzymalska K, Grebicka P, Mlynarczyk DT, Chełminiak-Dudkiewicz D, Kaczmarek H, Gośliński T, Ziegler-Borowska M; (2020) Crosslinking of chitosan with dialdehyde chitosan as a new approach for biomedical applications. Materials 13(15), 3413. **DOI:**10.3390/ma13153413

[28] Lin CY, Wang PH, Lee WN, Li WC, Wen TC; (2021) Chitosan with various degrees of carboxylation as hydrogel electrolyte for pseudo solid-state supercapacitors. J Power Sources 494, 229736. **DOI:**10.1016/j.jpowsour.2021.229736

[29] Takeshita S, Yoda S; (2017) Translucent, hydrophobic, and mechanically tough aerogels constructed from trimethylsilylated chitosan nanofibers. Nanoscale 9(34), 12311–12315. **DOI:**10.1039/c7nr04051b

[30] Zhang X, Wu D, Chu C; (2003) Effect of the crosslinking level on the properties of temperature-sensitive poly(N-isopropylacrylamide) hydrogels. J Polym Sci B 41(6), 582–593. **DOI:**10.1002/polb.10388

[31] Gajewski P, Żyła W, Kazimierczak K, Marcinkowska A; (2023) Hydrogel polymer electrolytes: synthesis, physicochemical characterization and application in electrochemical capacitors. Gels 9(7), 527. **DOI:**10.3390/gels9070527

[32] Zhang Q, Zhao L, Yang H, Kong L, Ran F; (2021) Alkali-tolerant polymeric gel electrolyte membrane based on cross-linked carboxylated chitosan for supercapacitors. J Mem Sci 629, 119083. **DOI:**10.1016/j.memsci.2021.119083

[33] Yang H, Ji X, Tan Y, Liu Y, Ran F; (2019) Modified supramolecular carboxylated chitosan as hydrogel electrolyte for quasi-solid-state supercapacitors. J Power Sources 441, 227174. **DOI:**10.1016/j.jpowsour.2019.227174

[34] Selvakumar M, Bhat DK; (2009) LiClO4-doped plasticized chitosan as biodegradable polymer gel electrolyte for supercapacitors. J Appl Polym Sci 114(4), 2445–2454. **DOI:**10.1002/app.30716

[35] Yang H, Liu Y, Kong L, Kang L, Ran F; (2019) Biopolymer-based carboxylated chitosan hydrogel film crosslinked by HCl as gel polymer electrolyte for all-solid-sate supercapacitors. J Power Sources 426, 47–54. **DOI:**10.1016/j.jpowsour.2019.04.023

[36] Na R, Huo G, Zhang S, Huo P, Du Y, Luan J, Zhu K, Wang G; (2016) A novel poly(ethylene glycol)-grafted poly(arylene ether ketone) blend micro-porous polymer electrolyte for solid-state electric double layer capacitors formed by incorporating a chitosan-based LiClO4 gel electrolyte. J Mater Chem A 4(46), 18116–18127. **DOI:**10.1039/c6ta07846j

[37] Nowacki K, Galiński M, Stępniak I; (2020) Synthesis and characterization of chitosan/sodium alginate blend membrane for application in an electrochemical capacitor. Prog Chem Appl Chitin Deriv 25, 174–191. **DOI:**10.15259/pcacd.25.014

[38] Taberna P, Simon P, Fauvarque J; (2003) Electrochemical characteristics and impedance spectroscopy studies of carbon-carbon supercapacitors. J Electrochem Soc 150(3), A292. **DOI:**10.1149/1.1543948

[39] Laschuk NO, Easton EB, Zenkina OV; (2021) Reducing the resistance for the use of electrochemical impedance spectroscopy analysis in materials chemistry. RSC Adv 11(45), 27925–27936. **DOI:**10.1039/d1ra03785d

[40] Hor AA, Hashmi S; (2020) Optimization of hierarchical porous carbon derived from a biomass pollen-cone as high-performance electrodes for supercapacitors. Electrochim Acta 356, 136826. **DOI:**10.1016/j.electacta.2020.136826

[41] Kasprzak D, Liu J; (2023) Chitin and cellulose as constituents of efficient, sustainable, and flexible zinc-ion hybrid supercapacitors. Sustain Mater Technol 38, e00726. **DOI:**10.1016/j.susmat.2023.e00726

[42] Yambou EP, Köps L, Kreth FA, Pohlmann S, Varzi A, Brousse T, Balducci A, Presser V; (2023) The many deaths of supercapacitors: degradation, aging, and performance fading. Adv Energy Mater 13(29), 2301008. **DOI:**10.1002/aenm.202301008

[43] Stępniak I, Galiński M, Nowacki K, Wysokowski M, Jakubowska P, Bazhenov VV, Leisegang T, Ehrlich H, Jesionowski T; (2016) A novel chitosan/sponge chitin origin material as a membrane for supercapacitors – preparation and characterization. RSC Adv 6(5), 4007–4013. **DOI:**10.1039/c5ra22047e

[44] Raja M, Balaji S, Ramavath JN, Dhamodharan R, Ramanujam K; (2019) A chitosan/poly(ethylene glycol)-ran-poly(propylene glycol) blend as an eco-benign separator and binder for quasi-solid-state supercapacitor applications. Sustain Energy Fuels 3(3), 760–773. **DOI:**10.1039/c8se00530c

[45] Zallouz S, Meins JL, Ghimbeu CM; (2022) Alkaline hydrogel electrolyte from biosourced chitosan to enhance the rate capability and energy density of carbon-based supercapacitors. Energy Adv 1(12), 1051–1064. **DOI:**10.1039/d2ya00250g